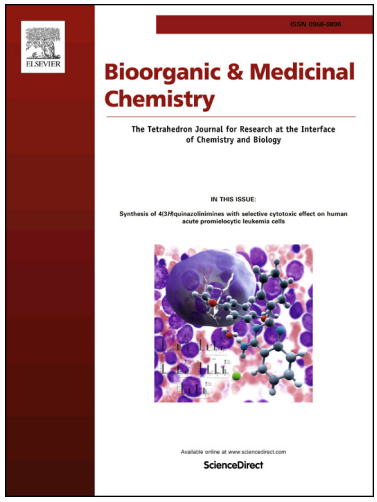

Discovery of BI 135585, an *in vivo* efficacious oxazinanone-based 11β hydroxysteroid dehydrogenase type 1 inhibitor

Linghang Zhuang, Colin M. Tice, Zhenrong Xu, Wei Zhao, Salvacion Cacatian, Yuan-Jie Ye, Suresh B. Singh, Peter Lindblom, Brian M. McKeever, Paula M. Krosky, Yi Zhao, Deepak Lala, Barbara A. Kruk, Shi Meng, Lamont Howard, Judith A. Johnson, Yuri Bukhtiyarov, Reshma Panemangalore, Joan Guo, Rong Guo, Frank Himmelsbach, Bradford Hamilton, Annette Schuler-Metz, Heike Schauerte, Richard Gregg, Gerard M. McGeehan, Katerina Leftheris, David A. Claremon

PII: S0968-0896(17)30593-X
DOI: http://dx.doi.org/10.1016/j.bmc.2017.04.033
Reference: BMC 13703

To appear in: *Bioorganic & Medicinal Chemistry*

Received Date: 27 March 2017
Revised Date: 24 April 2017
Accepted Date: 26 April 2017

Please cite this article as: Zhuang, L., Tice, C.M., Xu, Z., Zhao, W., Cacatian, S., Ye, Y-J., Singh, S.B., Lindblom, P., McKeever, B.M., Krosky, P.M., Zhao, Y., Lala, D., Kruk, B.A., Meng, S., Howard, L., Johnson, J.A., Bukhtiyarov, Y., Panemangalore, R., Guo, J., Guo, R., Himmelsbach, F., Hamilton, B., Schuler-Metz, A., Schauerte, H., Gregg, R., McGeehan, G.M., Leftheris, K., Claremon, D.A., Discovery of BI 135585, an *in vivo* efficacious oxazinanone-based 11β hydroxysteroid dehydrogenase type 1 inhibitor, *Bioorganic & Medicinal Chemistry* (2017), doi: http://dx.doi.org/10.1016/j.bmc.2017.04.033

Discovery of BI 135585, an *in vivo* efficacious oxazinanone-based 11β hydroxysteroid dehydrogenase type 1 inhibitor

Linghang Zhuang,*[,a] Colin M. Tice,[a] Zhenrong Xu,[a] Wei Zhao,[a] Salvacion Cacatian,[a] Yuan-Jie Ye,[a] Suresh B. Singh,[a] Peter Lindblom,[a] Brian M. McKeever,[b] Paula M. Krosky,[b] Yi Zhao,[b] Deepak Lala,[b] Barbara A. Kruk,[b] Shi Meng,[b] Lamont Howard,[b] Judith A. Johnson,[b] Yuri Bukhtiyarov,[b] Reshma Panemangalore,[b] Joan Guo,[b] Rong Guo,[b] Frank Himmelsbach,[c] Bradford Hamilton,[c] Annette Schuler-Metz,[c] Heike Schauerte,[c] Richard Gregg,[b] Gerard M. McGeehan,[b] Katerina Leftheris[a] and David A. Claremon[a]

[a] *Medicinal chemistry, Vitae Pharmaceuticals, Inc, 502West Office Center Drive, Fort Washington, Pennsylvania 19034, United States*

[b] *Biology, Vitae Pharmaceuticals, Inc, 502West Office Center Drive, Fort Washington, Pennsylvania 19034, United States*

[c] *Boehringer Ingelheim Pharma GmbH & Co. KG, 88400 Biberach, Germany*

RECEIVED DATE

To whom correspondence should be address.

Phone: +1 267 454-0795. Email: linghang_zhuang@yahoo.com.

Graphical Abstract

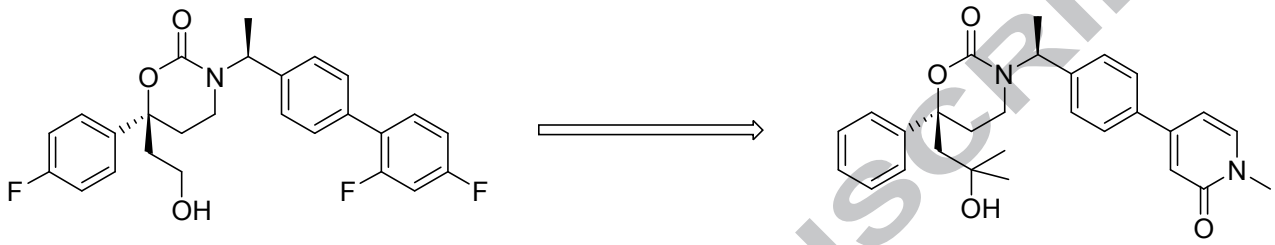

7 **11j**

Human adipocyte IC_{50}: 2.5 nM
Human adipose tissue IC_{80}: > 1000 nM
Log P 4.2

Human adipocyte IC_{50}: 4.3 nM
Human adipose tissue IC_{80}: 53 nM
Log P 2.6

ABSTRACT

A potent, *in vivo* efficacious 11β hydroxysteroid dehydrogenase type 1 (11β HSD1) inhibitor (**11j**) has been identified. Compound **11j** inhibited 11β HSD1 activity in human adipocytes with an IC_{50} of 4.3 nM and in primary human adipose tissue with an IC_{80} of 53 nM. Oral administration of **11j** to cynomolgus monkey inhibited 11β HSD1 activity in adipose tissue. Compound **11j** exhibited > 1000x selectivity over other hydroxysteroid dehydrogenases, displays desirable pharmacodynamic properties and entered human clinical trials in 2011.

KEYWORDS

11beta hydroxysteroid dehydrogenase type 1, inhibitor, oxazinanone, human adipocyte, human adipose tissue.

Introduction

Diabetes is an abnormal state marked by inability to make sufficient insulin or inability to appropriately respond to insulin, leading to the accumulation of glucose in blood and urine.[1] When left untreated, diabetes results in serious complications including cardiovascular disease, renal failure, and retinal damage and is often complicated by co-morbidities of obesity, dyslipidemia, and hypertension. Current therapies include life style intervention, oral anti-diabetes drugs, and injections of insulin or incretin mimetics, but the need for novel, safe, and easy to administer alternatives persists due to inadequate improvement in glycemic control and/or intolerable side effects.[2] Advances have been made in recent years to understand the fundamental biology underlying this assembly of diseases, collectively known as "metabolic syndrome," raising the opportunity for pharmacological intervention which directly impact their etiology and progression.

One enzyme proposed to be critical for the development of metabolic syndrome is 11β-hydroxysteroid dehydrogenase type 1 (11β-HSD1), a member of the short chain dehydrogenase/reductase (SDR) superfamily,[3-4] responsible for the local conversion of inactive cortisone to the active glucocorticoid cortisol. Cortisol binds to and activates the glucocorticoid receptor, resulting in increased expression of a wide range of genes involved in metabolism, immune response, bone formation, memory, and reproduction. More specifically, cortisol drives gluconeogenesis in the liver and adipogenesis in adipose tissue, which when elevated may contribute to metabolic syndrome. Circulating levels of cortisol are tightly controlled through multiple mechanisms; however, tissue-specific concentrations of cortisol vary from plasma levels primarily due to the expression and activity of 11β-HSD1.[5]

Multiple groups have pursued inhibitors of 11β-HSD1 as potential drugs for treatment of diabetes (Figure 1).[6] Carbenoxolone (**1**), the hemisuccinate derivative of natural product glycyrrhetinic acid, is a nonselective inhibitor of 11β-HSD1 and 11β-hydroxysteroid dehydrogenase type 2 (11β-HSD2). Despite its lack of selectivity for 11-βHSD1, **1** has been investigated in human studies where it enhanced hepatic insulin sensitivity.[7-8] Recently, two

groups have disclosed the effects of 11β-HSD1 inhibitors in Phase II trials in Type 2 diabetes patients. When added to ongoing metformin therapy, a 200 mg dose of INCB13739 (structure not disclosed) once daily for 12 weeks reduced HbA1c by 0.6% and fasting plasma glucose by 24 mg/dL.[9] A 6 mg/day dose of **2** (MK-0916) once daily for 12 weeks did not improve fasting plasma glucose; however, modest improvements in HbA1c, body weight and blood pressure were observed.[10] These studies support the hypothesis that a selective inhibitor of 11β-HSD1 may be useful in the treatment of diabetes and other morbidities associated with metabolic syndrome. Additional compounds have entered clinical trials.[6] Phase I results have been reported for aminothiazolone **3** (AMG-221)[11] and aminopyridine sulfonamide **4** (PF-915275).[12] Piperazine sulfonamide **5** (HSD-016)[13-14] and carboxylic acid **6** (AZ8329) have also completed Phase 1.[15]

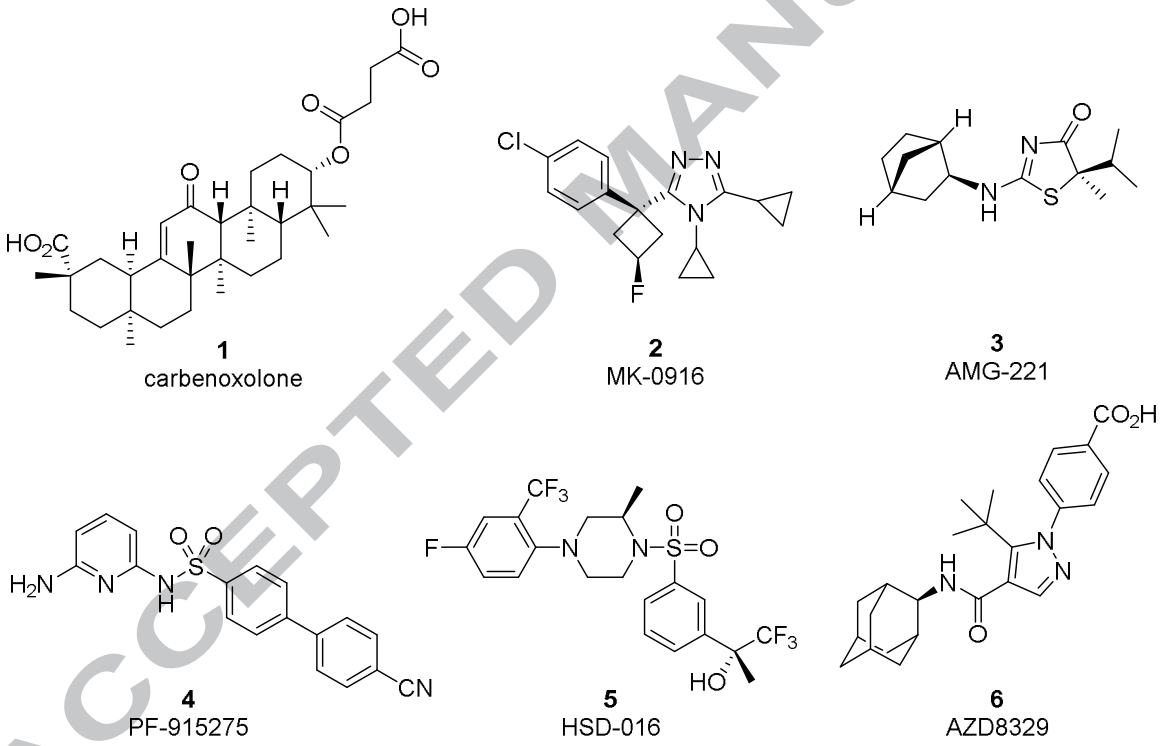

Figure 1. Selected 11β-HSD1 inhibitors that have entered clinical trials.

Recently, we reported potent oxazinanone-based 11β-HSD1 inhibitor **7** (Figure 2).[16] Compound **7** inhibited 11β-HSD1 with IC_{50} values of 0.8 nM in a biochemical assay and 2.0 nM in a cell-

based human adipocyte assay. It displayed > 1000x selectivity over 11β-HSD2 and two other related hydroxysteroid dehydrogenases. Further development of **7** was abandoned due to its lack of efficacy in an adipose tissue-specific, cynomolgus monkey PD study. Since **7** is very hydrophobic (log P 4.2) and highly protein bounded (> 99%), we reasoned that its unfavorable physical properties may have contributed to the loss of efficacy in the cyno PD study. We anticipated that a compound with improved physical properties would show a better correlation between *in vitro* and *in vivo* potency. Here we detail our efforts to reduce the hydrophobicity and increase the water solubility of **7**, leading to the discovery of a clinical candidate BI 135585 (**11j**).[17]

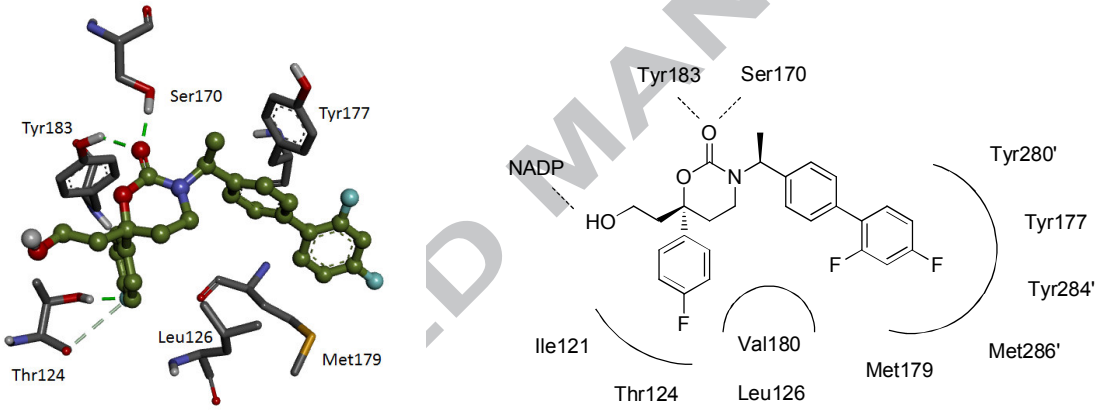

Figure 2. The structure of compound **7** and its proposed binding mode in the substrate binding site of human 11β-HSD1 (docked in 2IRW).

Lead optimization

A structure-based approach was adopted to optimize the physical chemical properties of **7**. A number of X-ray structures of 11β-HSD1 have been published.[18-19] In our work we employed the protein portion of the publicly available, homodimeric[20] structure deposited as PDB entry 2IRW.[21] The modeled pose of **7** in the 2IRW protein is depicted in Figure 2. The left hand side 4-fluorophenyl ring occupies a hydrophobic pocket formed by Ile121, Thr124, Leu126, and

Val180. The side chain hydroxyl group of **7** formed a hydrogen bond with one of the phosphate oxygens of the cofactor NADP and highlighted one region of the molecule where more polar substituents might be tolerated. The right hand side 2,4-difluorophenyl ring fits into a hydrophobic pocket shaped by Leu126, Val180, Met179, and Tyr177, as well as Met286', Tyr284' and Tyr280' (not shown for the clarity of picture) from the partner monomer. Since the 2,4-difluorophenyl ring is proximal to the interface of the two monomers, it seemed plausible that this hydrophobic ring could be replaced with more polar groups. A three-pronged approach was thus taken to reduce the hydrophobicity of **7** (Figure 3): 1) introduction of a basic nitrogen to permit salt formation; 2) removal of the 2, 4-difluorophenyl ring to reduce the molecular weight and number of aromatic rings, thereby increasing the ratio of polar surface area to total surface area; 3) replacement of the 2, 4-difluorophenyl ring with aromatic heterocycles.

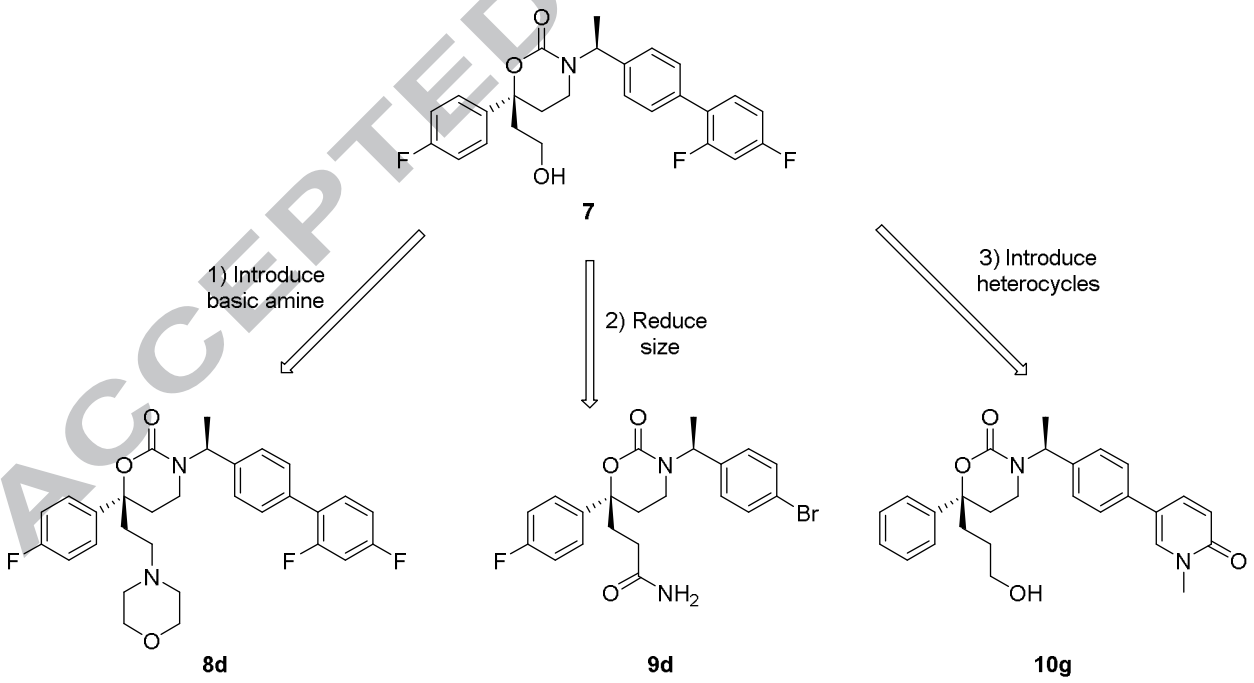

Figure 3. Selected analogs prepared as part of a three-pronged approach to improve the polarity of **7**.

Initially, we focused on the hydroxyethyl side chain because the model indicated that polar groups might be tolerated in that region. When the sidechain hydroxyl was replaced with a primary amine, the resulting compound **8a** was 3-fold less potent in the enzyme assay and 30-fold less potent in a cell-based adipocyte assay (Table 1). Changing the primary amine to secondary *N*-methyl amine **8b** further reduced potency in the enzyme assay. The tertiary *N,N*-dimethylamine **8c** was 3-fold less potent than the **8b**. However, a cyclic tertiary amine, morpholine **8d**, was 4-fold more potent than *N*-methyl amine **8b** and 16-fold more potent than the *N,N*-dimethylamine **8c**, suggesting that the basicity of the amine nitrogen in **8c** may contribute more to the loss of potency than steric effects. Although both **8d** and imidazolyl compound **8e** exhibited IC_{50} values < 5 nM in the enzyme assay, their cellular potencies (IC_{50} values of 48.7 and 19.8 nM, respectively) were unacceptable. Since none of the amine-containing compounds met our criteria for advancement, the first approach to reduce hydrophobicity was terminated.

Table 1. SAR of side chain amines

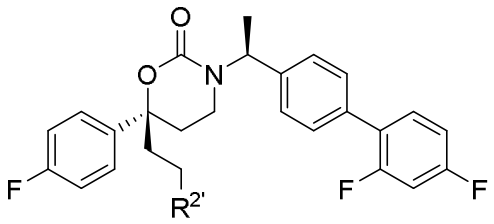

Compound	$R^{2'}$	Enzyme IC_{50}[a] (nM)	Adipocyte IC_{50}[a] (nM)
7	OH	0.8	2.5
8a	NH_2	2.7	66.5
8b	NHMe	23.6	244
8c	NMe_2	80	
8d	morpholine-4-yl	4.8	48.7
8e	1H-imidazol-1-yl	1.4	19.8

[a] Average of at least two replicates.

Explorations to reduce hydrophobicity and improve water solubility through reduction in molecular weight and the number of aromatic rings started with compound **9a** (Table 2), a synthetic precursor of **7**. Compound **9a** was a potent inhibitor of 11β-HSD1 with IC_{50} values of 1.7 and 3.0 nM in the enzyme and adipocyte assays, respectively. Addition of two methyl groups on the side chain led to a tertiary alcohol **9b**, which was 2-fold more potent in the enzyme assay and more stable in a rat liver microsome (RLM) incubation assay than the primary alcohol **9a**. Compound **9b**, however, inhibited recombinant CYP3A4 with an IC_{50} of 3.5 μM. Replacing the primary alcohol with a carboxamide (compound **9c**) resulted in a 4-fold loss of potency. However, homologous carboxamide **9d** regained potency in both the enzyme and adipocyte assays. Compound **9d** exhibited reasonable stability ($t_{1/2}$ 36 min) in RLM incubation and no inhibition of CYP3A4 up to 30 μM. Nitrile (**9e**) and sulfonamide (**9f**) groups in the side chain improved the potency. However, neither compound was sufficiently stable in RLM's for advancement.

The side chain amide **9d** was followed up with variations on the right (R^3) and left (R^1) hand side phenyl rings. When bromine on the right hand phenyl ring was replaced by fluorine, chlorine, trifluoromethyl, or nitrile (compounds **9g**, **9h**, **9j** and **9k**) groups, reductions in potency were observed. Replacing the bromine with methyl or methoxyl groups (compound **9i** and **9l**) retained potency in the adipocyte assay, but the compounds were unstable during RLM incubation. Consequently, difluoromethoxyl and trifluoromethoxyl groups were introduced to improve metabolic stability. The difluoromethoxyl analog (compound **9n**) showed an IC_{50} of 5.4 nM in adipocyte assay, was stable in RLM incubation ($t_{1/2}$ > 60 min), and only weakly inhibited CYP3A4 (IC_{50} 27 μM). The trifluoromethoxyl analog (compound **9m**) was less potent (IC_{50} 14.5 nM in the adipocyte assay). Removal of the fluorine from the left phenyl ring (R^1) of compound **9n** led to a 2-fold more potent compound **9o** in the adipocyte assay. Compound **9o** also had good RLM stability ($t_{1/2}$ 50.6 min) and a clean CYP3A4 profile (IC_{50} > 30 μM). Difluoromethoxyl analogs with tertiary alcohol side chains (compound **9p** and **9q**) also were prepared. While both compounds exhibited excellent potency and metabolic stability, they inhibited CYP3A4 with IC_{50} values of 6.6 and 10 μM, respectively.

Table 2. SAR of truncated right hand side compounds

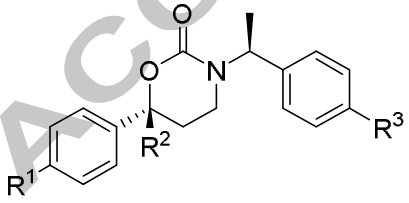

Cpd	R^1	R^2	R^3	Enzmye IC_{50} [a] (nM)	Adipocyte IC_{50} [a] (nM)	RLM $t_{1/2}$ (min)	CYP3A4 IC_{50} (μM)
9a	F	CH_2CH_2OH	Br	1.7	3.0	25	> 30

9b	F	$CH_2C(Me)_2OH$	Br	0.8	1.9	53.0	3.5
9c	F	$CH_2C(O)NH_2$	Br	7.7			
9d	F	$CH_2CH_2C(O)NH_2$	Br	1.1	3.0	36.1	> 30
9e	F	$CH_2C(Me)_2CN$	Br	0.8	0.8	20.3	
9f	F	$CH_2CH_2CH_2NHSO_2Me$	Br	0.7	0.7	11.4	
9g	F	$CH_2CH_2C(O)NH_2$	F	10.6	22.4		
9h	F	$CH_2CH_2C(O)NH_2$	Cl	2.3	12.9		
9i	F	$CH_2CH_2C(O)NH_2$	Me	2.2	4.7	7.1	
9j	F	$CH_2CH_2C(O)NH_2$	CF_3	3.6	35.0		
9k	F	$CH_2CH_2C(O)NH_2$	CN	65.9			
9l	F	$CH_2CH_2C(O)NH_2$	OMe	4.1	5.9	9.0	
9m	F	$CH_2CH_2C(O)NH_2$	OCF_3	2.9	14.5	> 60	
9n	F	$CH_2CH_2C(O)NH_2$	$OCHF_2$	2.0	5.4	> 60	27.0
9o	H	$CH_2CH_2C(O)NH_2$	$OCHF_2$	2.0	2.1	50.6	>30
9p	F	$CH_2C(Me)_2OH$	$OCHF_2$	1.2	5.7	> 60	6.6
9q	H	$CH_2C(Me)_2OH$	$OCHF_2$	1.3	0.7	>60	10

[a] Average of at least two replicates.

Based on in vitro potency, selectivity against the CYP enzymes, and stability during RLM incubation, **9d**, **9n**, **9o** and **9q** were selected for further profiling. These compounds had good aqueous solubility, ranging from 0.26 to 1.5 mg/mL, when tested as amorphous materials and were stable when incubated with human liver microsomes (Table 3). When dosed to rats intravenously, amides **9d** and **9n** exhibited acceptable mean residence times (MRT 1.2 and 0.84 h), albeit with high clearance rates of 49 and 67 mL/min/kg, respectively. Not surprisingly, the des-fluoro amide **9o** has a shorter mean residence time (MRT 0.55 h) and a higher clearance rate (91 mL/min/kg) than its fluorinated counterpart **9n**. The des-fluoro tertiary alcohol **9q**, however, showed a more moderate clearance rate of 23 mL/min/kg and an acceptable mean residence time of 0.84 h. All four compounds appeared to be absorbed readily in a rat pharmacokinetic (PK) study; bioavailability ranged from 42 to 77%. Further profiling revealed that amides **9d** and **9n** inhibited human *Ether-à-go-go*-Related Gene (hERG) potassium ion channel with IC_{50} values of 6.3 and 5.3 μM, respectively, and these four compounds were not pursued further.

Table 3. Profile of selected truncated analogs **9**

Compound	Aqueous Solubility (mg/mL)	HLM $t_{1/2}$ (min)	hERG IC_{50} (μM)	Rat PK		
				IV MRT (h)	IV CL (mL/min /kg)	F (%)
9d	0.30	> 90	6.3	1.2	49	42
9n	0.46	> 90	5.3	0.84	67	77
9o	1.5	> 90		0.55	91	51
9q	0.26	> 90		0.84	23	57

Our third approach to reduce logP was to replace the distal phenyl ring in **7** with polar heterocycles. Initial compounds were prepared with a hydroxypropyl sidechain (Table 4). All three pyridine regioisomers (**10a**, **10b**, and **10c**) showed IC_{50} < 1 nM in both enzyme and cell adipocyte assays. However, the 3- and 4- pyridinyl compounds, **10b** and **10c**, inhibited CYP3A4 with IC_{50} values of ~2 μM, while 2- pyridinyl compound **10a** only marginally inhibited CYP3A4 with IC_{50} of 23 μM. Presumably, the more hindered environment in compound **10a** prevented the pyridine nitrogen from interacting effectively with the heme iron in CYP3A4. The same phenomenon was observed with compound **10d**, a 2,6-dimethyl analog of **10c**, which did not show any CYP3A4 inhibition up to 30 μM. Decreasing the basicity of the pyridine nitrogen was also explored to alleviate CYP3A4 inhibition. The less basic fluoropyridine **10e** (CYP3A4 IC_{50} 10 μM) was less potent against CYP3A4 than its des-fluoro counterpart **10b** (CYP3A4 IC_{50} 2.1 μM). 2-Methoxypyridine **10f** did not inhibit CYP3A4 up to 30 μM, presumably due to synergy between electronic and steric effects. In addition, polar, but non-basic pyridinone **10g** was tolerated.

Table 4. SAR of pyridine analogs on the right hand side

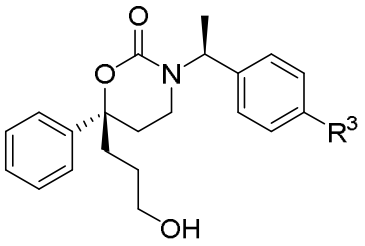

Compound	R^3	Enzmye IC_{50}[a] (nM)	Adipocyte IC_{50}[a] (nM)	CYP 3A4 IC_{50} (μM)
10a	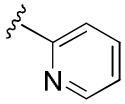	0.7	0.6	23 .3
10b	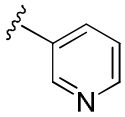	1.0	0.8	2.1
10c	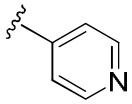	0.6	0.4	1.8
10d	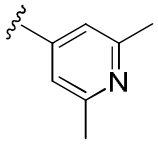	1.3	2.2	> 30
10e	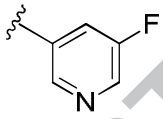	0.5	0.5	11.0
10f	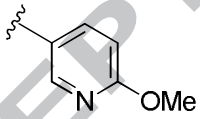	2.3	4	> 30
10g	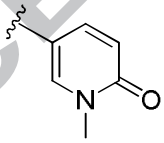	1.4	5.7	10.5

[a] Average of at least two replicates.

Although potent, these compounds generally were not stable to RLM incubation. For instance, **10d** has $t_{1/2}$ of 13 min in RLM. Identification of the metabolites generated during RLM

incubation implicated the propyl alcohol sidechain. To address this liability, analogs with tertiary alcohol side chains were prepared (Table 5). Compound **11a**, the tertiary alcohol counterpart of compound **10d**, exhibited IC_{50} values of 2.6 and 1.2 nM in enzyme and adipocyte assays, respectively. It was stable in RLM ($t_{1/2}$ > 45 min), although slightly less stable in microsomes from cynomolgus monkeys ($t_{1/2}$ 38 min). The 2-methoxypyridine **11b** was potent against 11β-HSD1 (IC_{50} 0.6 nM in enzyme assay), but inhibited CYP2C9 with an IC_{50} of 8 μM. The fluoro- and cyano- pyridine analogs (compounds **11c** and **11d**) were potent in the adipocyte assay and stable in liver microsome stability studies, but showed some inhibition of CYP3A4 (IC_{50} < 30 μM). The carboxamide **11e** represented a compound which was potent, stable in rat, monkey and human liver microsomes, and had a clean CYP profile (no inhibition up to 50 μM); however, **11e** had low bioavailability in rat (15%) and was not pursued further. Analogs with more electron deficient heterocycles, such as pyrazine (**11f**), pyridazine (**11g**) or pyrimidine (**11h**), combined potency with clean CYP profiles. While **11f** suffered from a short $t_{1/2}$ (16 min) in RLM incubation, **11g** and **11h** showed good stability in rat, cynomolgus monkey and human liver microsomes ($t_{1/2}$ > 45 min). The pyridinones **11i** and **11j** and pyridazinone **11k** also were potent inhibitors of 11β-HSD1. They exhibited clean CYP profiles (IC_{50} > 43 μM) and were stable in rat, cyno and human microsomes ($t_{1/2}$ > 90 min, except for compound **11k** in cynomolgus monkey microsome where $t_{1/2}$ > 45 min). The five member thiazole analog **11l** was less potent, with IC_{50} of 11.3 nM in the adipocyte assay. The bicyclic triazolopyridine **11m** inhibited CYP3A4 with an IC_{50} of 10 μM. Incorporation of aromatic heterocycles led to the identification of compounds **11g-k** which passed preliminary metabolic stability and drug-drug interaction screening.

Table 5. SAR of right hand side heterocycle compounds bearing tertiary alcohol side chain

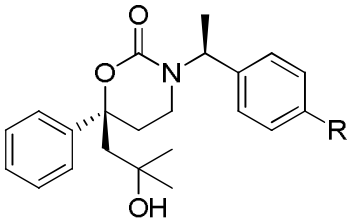

Cpd.	R	Enzmye IC_{50} [a] (nM)	Adipocyte IC_{50} [a] (nM)	CYPs IC_{50} (μM)			uSome Stability $t_{1/2}$ (min)		
				3A4	2D6	2C9	Rat	Cyno	Human
11a	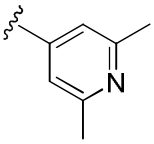	2.6	1.2	> 50	> 50	21.4	> 45	38	> 45
11b	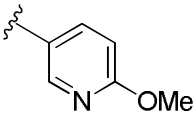	0.6	0.9	11.6	> 50	8			
11c	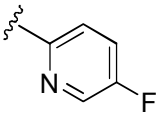	0.8	0.6	24.1	> 50	20.1	> 45	> 45	> 45
11d	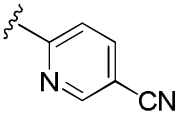	1.1	0.8	12.7	> 50	22.2	> 90	> 90	> 90
11e	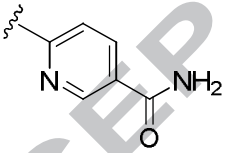	1.6	1.1	> 50	> 50	> 50	> 45	> 45	> 90
11f	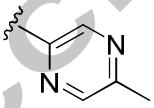	1.0	1.2	> 50	> 50	33	16	38	> 90
11g	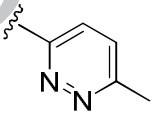	1.2	2.5	> 50	> 50	> 50	> 45	> 45	> 90
11h	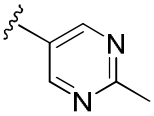	2.5	3.7	> 50	> 50	> 50	> 90	> 90	> 90
11i	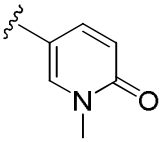	1.6	3.3	48	> 50	43	> 90	> 90	> 90

11j	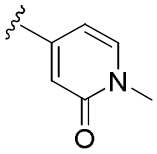	1.7	4.3	> 50	> 50	> 50	> 90	> 90	> 90
11k	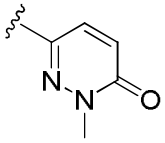	1.8	1.0	> 50	> 50	> 50	> 90	> 45	> 90
11l	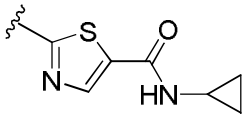	1.7	12.3						
11m	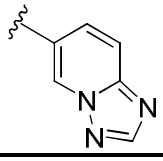	1.4	3.8	10	> 50	> 50	> 90	> 45	> 90

[a] Average of at least two replicates.

Compound selection

The failure of prototype compound **7** to show reasonable inhibition of 11β-HSD1 enzyme activity in the adipose tissues of acutely dosed cynomolgus monkeys, prompted the development of a novel assay to identify compounds more likely to succeed in vivo. To this end, an *in vitro* assay was developed using primary human adipose tissue collected during surgery. Tissue fragments were incubated in cell culture media +/- selected compounds and the conversion of cortisone to cortisol was measured.[17] Compound **7** had an $IC_{80} > 1$ μM in this assay, consistent with minimal efficacy in the monkey pharmacodynamic (PD) study. Thus an $IC_{80} \leq 100$ nM in this assay was set as criteria for new compounds to advance to in vivo analysis. Other criteria included selectivity against the hERG channel and good PK in non-human primates.

The five previously selected compounds **11g-k** were filtered with these criteria. All five compounds met the human adipose tissue criterion and two (**11g** and **11j**) exceeded it (Table 6). A patch-clamp assay for hERG was performed at 10 μM; 50% and 12% hERG inhibition values were observed with compounds **11k** and **11h** respectively, while **11g**, **11i** and **11j** did not significantly inhibit hERG (< 10%). When administered intravenously to cynomolgus monkeys, **11g-j** showed low clearance rates and good exposure (Table 6). Compound **11j** had the best potency in the adipose tissue assay, did not inhibit hERG, exhibited the longest MRT in cynomolgus monkeys, and was therefore chosen for further characterization.

Table 6. Inhibition of 11β-HSD1 in human adipose tissue, hERG and cyno PK for selected compounds

Compound	Adipose tissue IC_{80} [a] (nM)	Inhibition of hERG at 10μM (%)	Cyno IV				Cyno PO	
			dnAUC (nMh)	MRT (h)	CL (mL/min/kg)	Vss (L/kg)	MRT (h)	F (%)
11g	76	< 10	3330	4.8	5.2	1.5	5.3	70
11h	100	12	2070	3.5	8.1	1.7	4.8	96
11i	100	< 10	1770	2.7	11	1.7	4.8	39
11j	53	< 10	2500	5.5	7.5	2.5	8.7	54
11k	100	50						

[a] Average of at least two replicates.

Further characterization

Compound **11j** was further screened against three related hydroxysteroid dehydrogenases and for other off target activities (Table 7). It exhibited > 1000x selectivity over 11β-HSD2, 3β-hydroxysteroid dehydrogenase type 2 (3β-HSD2), 17β-hydroxysteroid dehydrogenase type 1 (17β-HSD1) and pregnane X receptor (PXR). Moreover, there were no significant findings in

the SpectrumScreen of 168 assays (Ricerca) when tested at 10 μM. Compound **11j** also was retested against the hERG channel and exhibited an IC_{50} > 100 μM. Regarding physical properties, **11j** had a measured logP of 2.6 and a human plasma protein binding of 91.6%, representing a significant improvement over compound **7** (log P 4.2, protein binding > 99%). The measured water solubility of **11j** was 0.22 mg/mL, whereas the water solubility of **7** was below the limit of detection. Compound **11j** was docked in the substrate binding site of human 11β-HSD1 (2IRW, Figure 4). It adopted similar binding mode as that of compound **7**, with the polar pyridone group pointing to the dimer interface. This binding mode supported the outcome that compound **11j** maintained potency, since the interface region was expected to be more tolerable to polar groups.

Table 7. Further characterization of **11j**

11β-HSD2 IC_{50} (μM)	>10
3β-HSD2 IC_{50} (μM)	>10
17β-HSD1 IC_{50} (μM)	>10
PXR EC_{50} (μM)	>10
SpectrumScreen (168 assays) IC_{50} (μM)	>10
Log P	2.6
Plasma protein binding (%, human)	91.6
Hepatocyte CL (mL/min/kg, human)	0.2
hERG IC_{50} (μM)	> 100

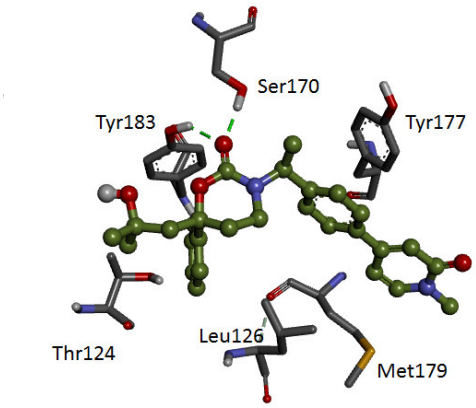

Figure 4. The docked binding pose of compound **11j** in the substrate binding site of human 11β-HSD1 (docked in 2IRW).

Cynomolgus monkey PD study

As described elsewhere, compound **11j** was further evaluated in a cynomolgus monkey PD model measuring conversion of cortisone to cortisol, *ex vivo*.[17] Briefly, treatment with **11j** at doses of 1 mg/kg and 3 mg/kg po, inhibited 67% and 90% of enzyme activity respectively in perirenal adipose tissue. In abdominal subcutaneous adipose tissue, 67% and 95% reductions of cortisol were observed, relative to vehicle treated animals. Thus, **11j** is effective in lowering 11β-HSD1 activity in adipose tissues in non-human primates when dosed orally. After successfully completing safety assessment, **11j** entered human clinical trials in 2011.

Chemistry

Compounds of general structure **8** (Table 1) were prepared as shown in Scheme 1. The primary hydroxyl group in compound **7** was mesylated, displaced with sodium azide and reduced with triphenylphosphine to give primary amine **8a**. Boc protection of **8a,** followed by methylation of the resultant carbamate, and deprotection, provided methylamine **8b**. Heating **8a** with formaldehyde and formic acid gave dimethylamine **8c**. The mesylate of compound **7** could also be directly displaced with morpholine or imidazole to give compound **8d** and **8e**.

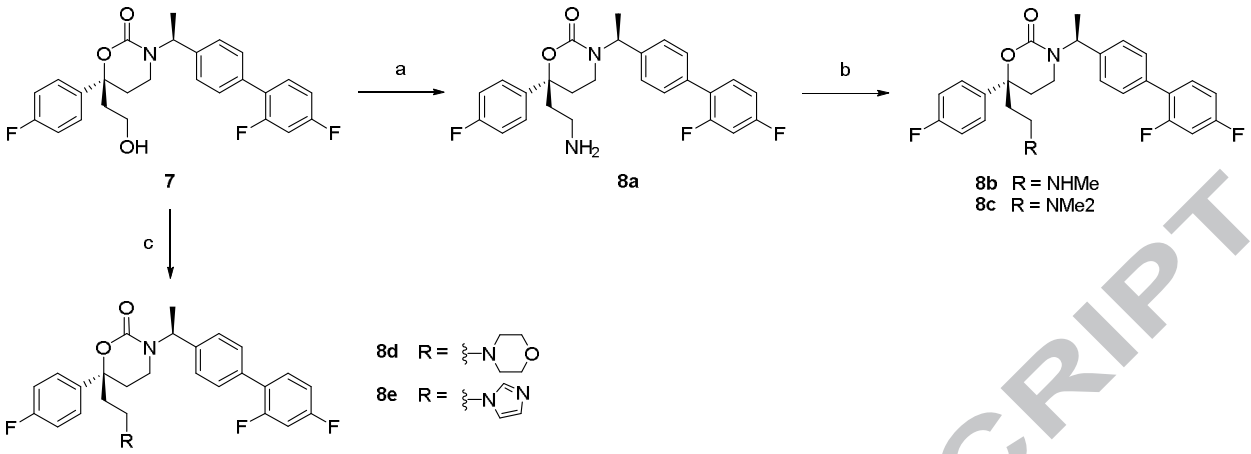

Scheme 1. Synthesis of side chain amine **8**.

Reagents and conditions. [a] (i) MsCl, Et_3N, CH_2Cl_2, 0 °C to rt; (ii) NaN_3, DMF, 70 °C; (iii) PPh_3, 20:1 THF/H_2O, rt; [b] For **8b** (i) Boc_2O, Et_3N, CH_2Cl_2, 0 °C to rt; (ii) NaH, MeI, THF, 0 °C to rt; (iii) 20% TFA/ CH_2Cl_2, 0 °C; For **8c** HCHO, HCO_2H, 90 °C; [c] (i) MsCl, Et_3N, CH_2Cl_2, 0 °C to rt; (ii) For **8d** morpholine, Et_3N, CH_2Cl_2, 0 °C to rt; For **8e**: imidazole, K_2CO_3, MeCN, reflux.

Compound **9a** (Table 2) was prepared as described previously.[16] Preparations of other compounds of general structure of **9** are depicted in Scheme 2. Compounds **9b**, **9p** and **9q** were prepared from the respective allyl oxazinanones **12b**, **12p** and **12q.** [16] The allyl oxazinanones were subjected to Wacker oxidation to give inseparable mixtures of methyl ketone **13** and aldehydes. The mixtures were then treated with sodium chlorite which oxidized the aldehydes to carboxylic acids which were soluble in the aqueous layer, allowing separation from **13**. Methyl Grignard addition to ketone **13** provided tertiary alcohols **9b, 9p** and **9q**. Compound **9c** was prepared from **12b** via a sequence of dihydroxylation, oxidative cleavage of the resultant diol to an acid and amide coupling. Hydroboration of **12b** provided alcohol **15b**, which was oxidized to the carboxylic acid and coupled with ammonia to give carboxamide **9d**. Compounds **9g-o** were prepared using the same reaction sequence used for **9d**. Cobalt catalyzed hydrocyanation of

olefin **12b** provided nitrile **16**, which upon methylation gave gem-dimethylnitrile **9e**. Compound **9f** was obtained from alcohol **15b** via mesylation then methanesulfonamide displacement. Compounds with general structure of **10** (Table 4) were prepared according to Scheme 3. Hydroboration of olefin **12a** provided propylalcohol **15a**, which was converted to boronic ester **18**. Suzuki coupling of bromide **15a** with various heteroaryl boronic acids or **18** with various heterocyclic halides gave compounds **10a-g**. Similarly, compounds **11a-m** (Table 5) were prepared by Suzuki couplings with bromide **9r** or boronic ester **19** (Scheme 5). Following the selection of **11j** as a clinical candidate an enantioselective synthesis was developed.[22]

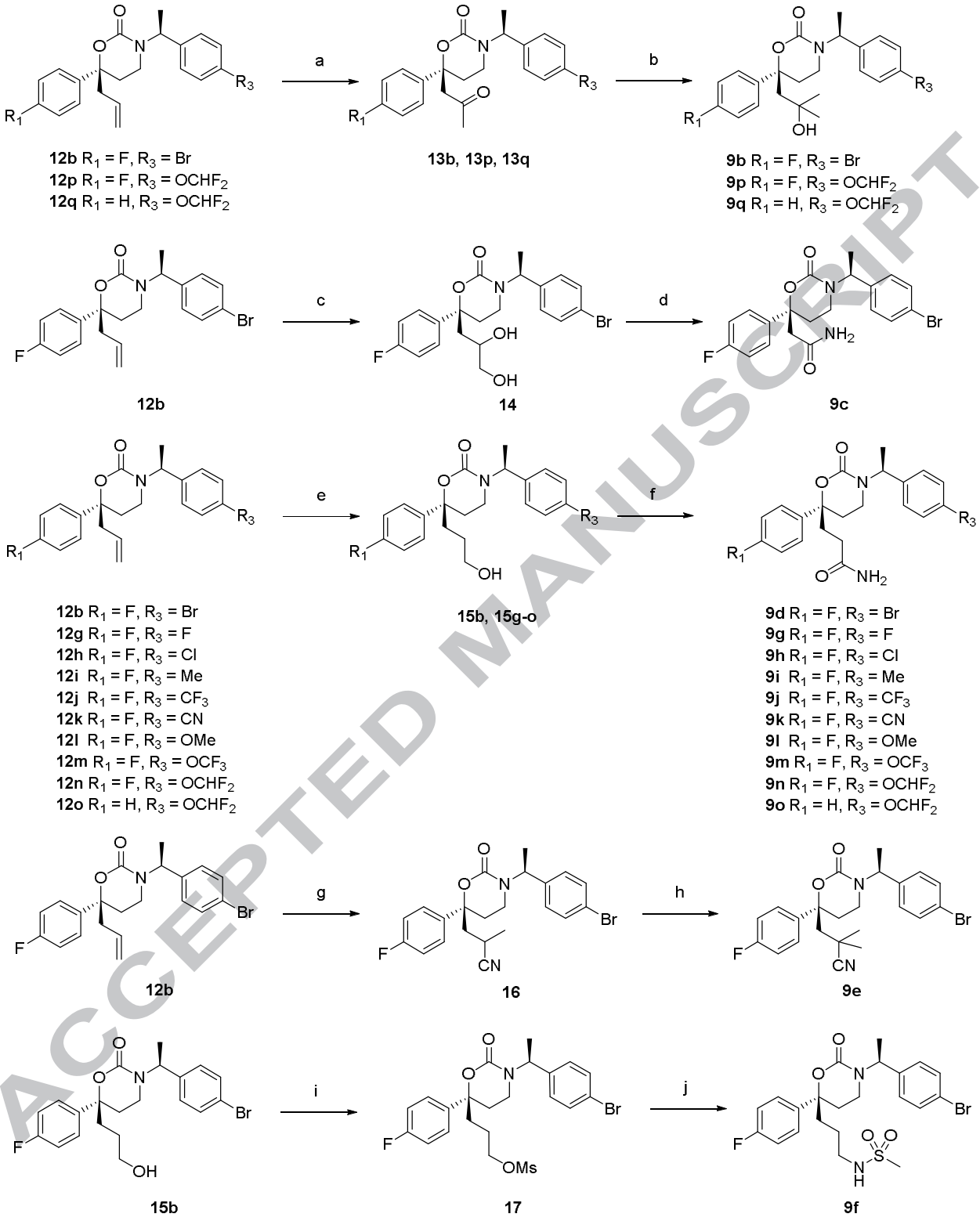

Scheme 2. Synthesis of truncated right hand side compounds **9**.

Reagents and conditions. [a] (i) $PdCl_2$, CuCl, O_2, DMF, H_2O, rt; (ii) $NaClO_2$, NaH_2PO_4, 2-methyl-2-butene, *t*-BuOH, H_2O; [b] MeMgBr, THF, -78 °C; [c] OsO_4, NMO, *t*-BuOH, CH_2Cl_2, rt; [d] (i) $RuCl_3$, Oxone, $NaHCO_3$, H_2O/CH_3CN/EtOAc, rt; (ii) HATU, NH_3, DIPEA, DMF, rt; [e] (i) BH_3THF, THF, 0 °C; (ii) NaOH, H_2O_2, rt; ; [f] CrO_3, H_2SO_4, H_2O/acetone, 0 °C; [g] [*N,N'*-(1,1,2,2-tetramethylethylene)bis(3,5-di-*tert*-butylsalicylideneiminato)]cobalt(II), TsCN, $PhSiH_3$, EtOH, rt; [h] LiHMDS, MeI, THF, -78 °C; [i] MsCl, Et_3N, CH_2Cl_2, 0 °C to rt; [j] $MeSO_2NH_2$, K_2CO_3, CH_3CN, rt.

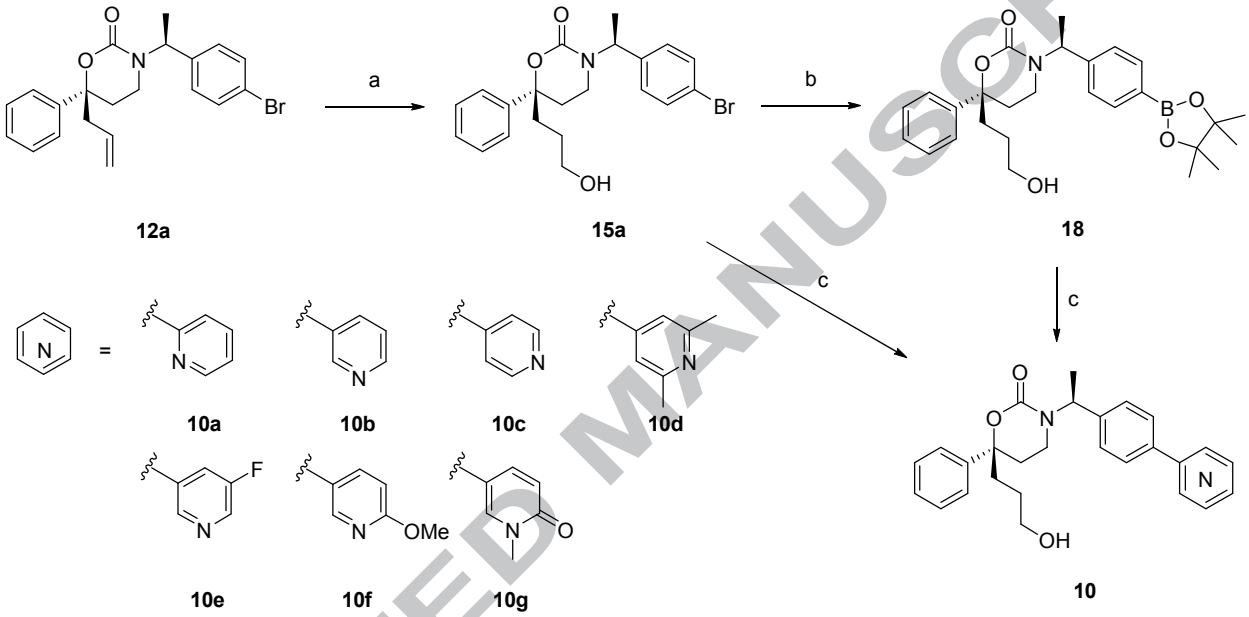

Scheme 3. Synthesis of right hand side heterocycle compounds **10**.

Reagents and conditions. [a] (i) BH_3.THF, THF, 0 °C; (ii) NaOH, H_2O_2, rt; [b] $PdCl_2$, pinacolborane, KOAc, DMSO, 90 °C; [c] $Pd(PPh_3)_2Cl_2$, ArBr or $ArB(OH)_2$, Cs_2CO_3, 1,4-dioxane, 120 °C.

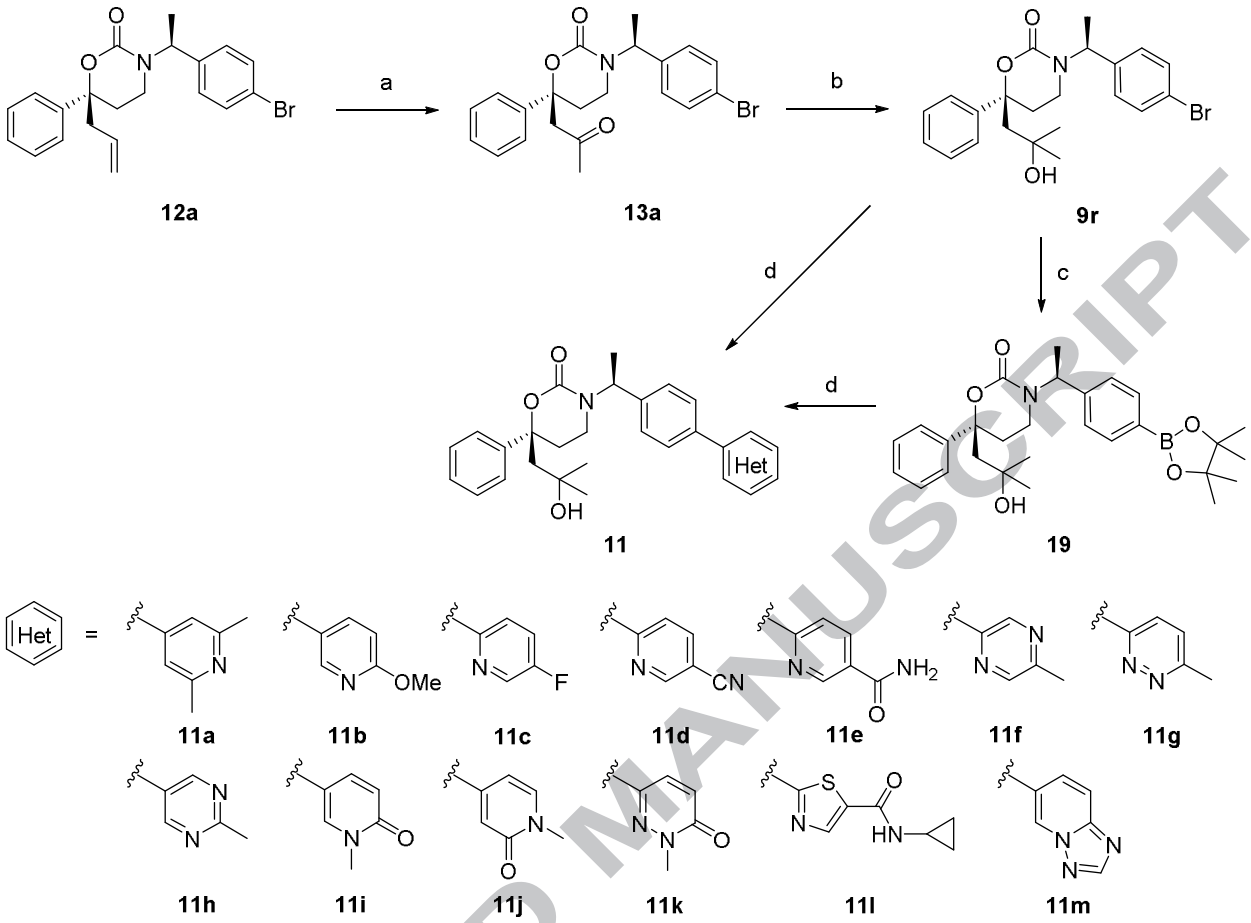

Scheme 4. Synthesis of right hand side heterocycle compounds **11**.

Reagents and conditions. Reagents and conditions. [a] (i) $PdCl_2$, CuCl, O_2, DMF, H_2O, rt; (ii) $NaClO_2$, NaH_2PO_4, 2-methyl-2-butene, *t*-BuOH, H_2O; [b] MeMgBr, THF, -78 °C; [c] $PdCl_2$, pinacolborane, KOAc, DMSO, 90 °C;[d] $Pd(PPh_3)_2Cl_2$, ArX or $ArB(OH)_2$, Cs_2CO_3, 1,4-dioxane, 120 °C.

Conclusion

We have described our efforts to improve the efficacy of compound **7** through modulation of its physical properties. To this end, we have successfully introduced polar groups into **7** and identified **11j** which has lower hydrophobicity (log P 2.6) and protein binding (91.6%). Compound **11j** is a potent inhibitor of 11β-HSD1 in human adipocytes with > 1000x selectivity over three other hydroxysteroid dehydrogenases, including 11β-HSD2. More importantly, **11j**

inhibits the conversion of cortisone to cortisol in primary human adipose tissue with IC_{80} values of 53 nM, compared to $IC_{80} > 1$ μM for **7**. Oral administration of **11j** to cynomolgus monkey inhibited 11β-HSD1 activity in adipose tissues. Compound **11j** displays desirable pharmacodynamic properties, meets safety assessment criteria, and entered human clinical trials in 2011.

Supporting Information Available

Synthetic procedures as well as NMR and LC-MS data on new compounds; assay protocols.

1. World Health Organization Global report on diabetes. http://www.who.int/diabetes/global-report/en/ (accessed 02/15/2017).
2. Mohler, M. L.; He, Y.; Wu, Z.; Hwang, D. J.; Miller, D. D., Recent and emerging anti-diabetes targets. *Med. Res. Rev.* **2009,** *29*, 125-195.
3. Tanaka, N.; Nonaka, T.; Nakamura, K. T.; Hara, A., SDR: structure, mechanism of action, and substrate recognition. *Curr. Org. Chem.* **2001,** *5*, 89-111.
4. Bray, J. E.; Marsden, B. D.; Oppermann, U., The human short-chain dehydrogenase/reductase (SDR) superfamily: A bioinformatics summary. *Chem.-Biol. Interact.* **2009,** *178*, 99-109.
5. Walker, B. R.; Andrew, R., Tissue production of cortisol by 11beta-hydroxysteroid dehydrogenase type 1 and metabolic disease. *Ann. N. Y. Acad. Sci.* **2006,** *1083*, 165-184.
6. Scott, J. S.; Goldberg, F. W.; Turnbull, A. V., Medicinal Chemistry of Inhibitors of 11β-Hydroxysteroid Dehydrogenase Type 1 (11β-HSD1). *J. Med. Chem.* **2014,** *57*, 4466-4486.
7. Walker, B. R.; Connacher, A. A.; Lindsay, R. M.; Webb, D. J.; Edwards, C. R. W., Carbenoxolone increases hepatic insulin sensitivity in man: a novel role for 11-oxosteroid reductase in enhancing glucocorticoid receptor activation. *J. Clin. Endocrinol. Metab.* **1995,** *80*, 3155-9.
8. Taylor, A.; Irwin, N.; McKillop, A. M.; Flatt, P. R.; Gault, V. A., Sub-chronic administration of the 11beta -HSD1 inhibitor, carbenoxolone, improves glucose tolerance and insulin sensitivity in mice with diet-induced obesity. *Biol. Chem.* **2008,** *389*, 441-445.
9. Rosenstock, J.; Banarer, S.; Fonseca, V. A.; Inzucchi, S. E.; Sun, W.; Yao, W.; Hollis, G.; Flores, R.; Levy, R.; Williams, W. V.; Seckl, J. R.; Huber, R., The 11-beta-hydroxysteroid dehydrogenase type 1 inhibitor INCB13739 improves hyperglycemia in patients with type 2 diabetes inadequately controlled by metformin monotherapy. *Diabetes Care* **2010,** *33*, 1516-1522.

10. Feig, P. U.; Shah, S.; Hermanowski-Vosatka, A.; Plotkin, D.; Springer, M. S.; Donahue, S.; Thach, C.; Klein, E. J.; Lai, E.; Kaufman, K. D., Effects of an 11β-hydroxysteroid dehydrogenase type 1 inhibitor, MK-0916, in patients with type 2 diabetes mellitus and metabolic syndrome. *Diabetes, Obes. Metab.* **2011,** *13*, 498-504.
11. Gibbs, J. P.; Emery, M. G.; McCaffery, I.; Smith, B.; Gibbs, M. A.; Akrami, A.; Rossi, J.; Paweletz, K.; Gastonguay, M. B.; Bautista, E.; Wang, M.; Perfetti, R.; Daniels, O., Population pharmacokinetic/pharmacodynamic model of subcutaneous adipose 11.beta -hydroxysteroid dehydrogenase type 1 (11.beta -HSD1) activity after oral administration of AMG 221, a selective 11.beta -HSD1 inhibitor. *Journal of Clinical Pharmacology* **2011,** *51*, 830-841.
12. Courtney, R.; Stewart, P. M.; Toh, M.; Ndongo, M.-N.; Calle, R. A.; Hirshberg, B., Modulation of 11beta -Hydroxysteroid dehydrogenase (11beta HSD) activity biomarkers and pharmacokinetics of PF-00915275, a selective 11beta HSD1 inhibitor. *J. Clin. Endocrinol. Metab.* **2008,** *93*, 550-556.
13. Wan, Z.-K.; Chenail, E.; Li, H.-Q.; Kendall, C.; Wang, Y.; Gingras, S.; Xiang, J.; Massefski, W. W.; Mansour, T. S.; Saiah, E., Synthesis of potent and orally efficacious 11.beta -hydroxysteroid dehydrogenase type 1 inhibitor HSD-016. *J. Org. Chem.* **2011,** *76*, 7048-7055.
14. Wan, Z. K. *Development of HSD-016 and HSD-621 as potential agents for the treatment of type 2 diabetes*, 4th World Congress on Diabetes & Metabolism, Chicago, IL, August 14-16; 2013.
15. Wang, Y.; Zhang, Y.; Wang, X.; Liu, Y.; Xia, M., Cyanidin-3-O-β-glucoside induces oxysterol efflux from endothelial cells: Role of liver X receptor alpha. *Atherosclerosis (Amsterdam, Neth.)*, Ahead of Print.
16. Xu, Z.; Tice, C. M.; Zhao, W.; Cacatian, S.; Ye, Y.-J.; Singh, S. B.; Lindblom, P.; McKeever, B. M.; Krosky, P. M.; Kruk, B. A.; Berbaum, J.; Harrison, R. K.; Johnson, J. A.; Bukhtiyarov, Y.; Panemangalore, R.; Scott, B. B.; Zhao, Y.; Bruno, J. G.; Togias, J.; Guo, J.; Guo, R.; Carroll, P. J.; McGeehan, G. M.; Zhuang, L.; He, W.; Claremon, D. A., Structure-Based Design and Synthesis of 1,3-Oxazinan-2-one Inhibitors of 11.beta -Hydroxysteroid Dehydrogenase Type 1. *J. Med. Chem.* **2011,** *54*, 6050-6062.
17. Hamilton, B. S.; Himmelsbach, F.; Nar, H.; Schuler-Metz, A.; Krosky, P.; Guo, J.; Guo, R.; Meng, S.; Zhao, Y.; Lala, D. S.; Zhuang, L.; Claremon, D. A.; McGeehan, G. M., Pharmacological characterization of the selective 11β-hydroxysteroid dehydrogenase 1 inhibitor, BI 135585, a clinical candidate for the treatment of type 2 diabetes. *European Journal of Pharmacology* **2015,** *746*, 50-55.
18. Singh, S. B.; Tice, C. M., Structure based design of 11beta -HSD1 inhibitors. *Current Pharmaceutical Biotechnology* **2010,** *11*, 779-791.
19. Thomas, M. P.; Potter, B. V. L., Crystal structures of 11.beta -hydroxysteroid dehydrogenase type 1 and their use in drug discovery. *Future Medicinal Chemistry* **2011,** *3*, 367-390.
20. Maser, E.; Voelker, B.; Friebertshaeuser, J., 11beta -Hydroxysteroid Dehydrogenase Type 1 from Human Liver: Dimerization and Enzyme Cooperativity Support Its Postulated Role as Glucocorticoid Reductase. *Biochemistry* **2002,** *41*, 2459-2465.
21. Patel, J. R.; Shuai, Q.; Dinges, J.; Winn, M.; Pliushchev, M.; Fung, S.; Monzon, K.; Chiou, W.; Wang, J.; Pan, L.; Wagaw, S.; Engstrom, K.; Kerdesky, F. A.; Longenecker, K.; Judge, R.; Qin, W.; Imade, H. M.; Stolarik, D.; Beno, D. W. A.; Brune, M.; Chovan, L. E.; Sham, H. L.; Jacobson, P.; Link, J. T., Discovery of adamantane ethers as inhibitors of 11beta-HSD-1: Synthesis and biological evaluation. *Bioorg. Med. Chem. Lett.* **2007,** *17*, 750-755.

22. Zhang, Y.; Wu, J.-P.; Li, G.; Fandrick, K. R.; Gao, J.; Tan, Z.; Johnson, J.; Li, W.; Sanyal, S.; Wang, J.; Sun, X.; Lorenz, J. C.; Rodriguez, S.; Reeves, J. T.; Grinberg, N.; Lee, H.; Yee, N.; Lu, B. Z.; Senanayake, C. H., An Enantioselective Synthesis of an 11-β-HSD-1 Inhibitor via an Asymmetric Methallylation Catalyzed by (S)-3,3′-F2-BINOL. *The Journal of Organic Chemistry* **2016,** *81*, 2665-2669.